Insights into Hydrogen Bonding and Stacking Interactions in Cellulose

ARTICLE *in* THE JOURNAL OF PHYSICAL CHEMISTRY A · DECEMBER 2011

Impact Factor: 2.69 · DOI: 10.1021/jp203620x · Source: PubMed

6 AUTHORS, INCLUDING:

R. Parthasarathi
Joint BioEnergy Institute
93 PUBLICATIONS **2,337** CITATIONS
SEE PROFILE

Giovanni Bellesia
University of California, Santa Barbara
26 PUBLICATIONS **567** CITATIONS
SEE PROFILE

Shishir Chundawat
Rutgers, The State University of New Jersey
66 PUBLICATIONS **2,073** CITATIONS
SEE PROFILE

Bruce E Dale
Michigan State University
333 PUBLICATIONS **11,000** CITATIONS
SEE PROFILE

THE JOURNAL OF PHYSICAL CHEMISTRY A

ARTICLE

pubs.acs.org/JPCA

Insights into Hydrogen Bonding and Stacking Interactions in Cellulose

R. Parthasarathi,[†] G. Bellesia,[†,‡] S. P. S. Chundawat,[§,¶] B. E. Dale,[§,¶] P. Langan,[⊥,∥] and S. Gnanakaran*[,†]

[†]Theoretical Biology & Biophysics Group, [‡]Center for Nonlinear Studies, [⊥]Bioscience Division, Los Alamos National Laboratory, Los Alamos, New Mexico 87545, United States

[§]Great Lakes Bioenergy Research Center, East Lansing, Michigan 48824, United States

[¶]Department of Chemical Engineering and Materials Science, Michigan State University, East Lansing, Michigan 48824, United States

[∥]Oak Ridge National Laboratory, Oak Ridge, Tennessee 37831-6475, United States

Supporting Information

ABSTRACT: In this quantum chemical study, we explore hydrogen bonding (H-bonding) and stacking interactions in different crystalline cellulose allomorphs; namely, cellulose I_β and cellulose III_I. We consider a model system representing a cellulose crystalline core made from six cellobiose units arranged in three layers with two chains per layer. We calculate the contributions of intrasheet and intersheet interactions to the structure and stability in both cellulose I_β and cellulose III_I crystalline cores. Reference structures for this study were generated from molecular dynamics simulations of water-solvated cellulose I_β and III_I fibrils. A systematic analysis of various conformations describing different mutual orientations of cellobiose units is performed using the hybrid density functional theory with the M06-2X with 6-31+G(d,p) basis sets. We dissect the nature of the forces that stabilize the cellulose I_β and cellulose III_I crystalline cores and quantify the relative strength of H-bonding and stacking interactions. Our calculations demonstrate that individual H-bonding interactions are stronger in cellulose I_β than in cellulose III_I; however, the total H-bonding contribution to stabilization is larger in cellulose III_I because of the highly cooperative nature of the H-bonding network. In addition, we observe a significant contribution from cooperative stacking interactions to the stabilization of cellulose I_β. The theory of atoms-in-molecules (AIM) has been employed to characterize and quantify these intermolecular interactions. AIM analyses highlight the role of nonconventional CH···O H-bonding in the cellulose assemblies. Finally, we calculate molecular electrostatic potential maps for the cellulose allomorphs that capture the differences in chemical reactivity of the systems considered in our study.

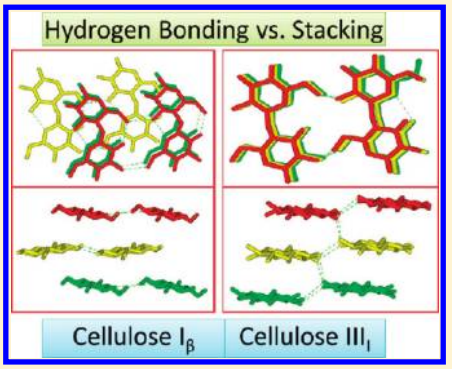

INTRODUCTION

Noncovalent interactions play a central role in stabilizing three-dimensional structures of biomacromolecules and are involved in the regulation of several biomolecular processes, such as enzyme−substrate binding, antibody−antigen recognition, biomolecular self-assembly, and formation of supramolecular structures.[1−4] Among noncovalent interactions, hydrogen bonding (H-bonding) and stacking interactions have been extensively studied in both nucleic acids and proteins as well as in their complexes.[2,5−13] In particular, stacking interactions have been characterized in biomolecules (purine and pyrimidine bases, aromatic amino acid side chains, and some of these in complexes with ligands)[8,9,13−23] and in complexes of organic molecules (benzene, phenol, etc.).[21,24−29] Recently, aromatic-carbohydrate stacking[30] and base-carbohydrate stacking have been analyzed by NMR experiments coupled with MD simulations.[31] For a long time, it was widely assumed that H-bonding interactions were much stronger than stacking interactions, and therefore, it was anticipated that H-bonding was the key player in determining biomolecular structure and function.[2] However, recent accurate quantum chemical calculations have shown that the stabilization provided by both types of noncovalent interactions can be comparable,[7,14] although H-bonding originates from electrostatics and charge transfer, whereas stacking is typically governed by van der Waals (vdW) interactions (comprising London dispersion), $\pi-\pi$ interactions, and hydrophobic forces.[2,8]

With respect to carbohydrate−carbohydrate interactions,[32] however, only the role of H-bonding has been explored; stacking interactions have yet to be fully quantified. Recent focus on producing biofuels by breaking down cellulosic biomass into fermentable sugars has increased interest in characterizing such interactions in carbohydrates. Cellulose is synthesized at the plasma membrane as a linear polymer of $\beta(1-4)$-linked D-glucose units. Cellulose polymer chains are assembled in H-bonded sheets that stack on top of each other to generate crystalline nanofibrils.[33]

Received: April 18, 2011
Revised: September 27, 2011
Published: October 24, 2011

Cellulose occurs naturally in two different crystal forms, namely, I_α and I_β, collectively referred to as cellulose I, which differ in the relative stagger of the stacked sheets. Cellulose in lignocellulosic biomass derived from the cell walls of higher plants is found mostly in the I_β form. Under carefully controlled pretreatment conditions using liquid ammonia (or other amines), the cellulose I_β crystal structure can be converted to a different crystalline form called cellulose III_I. X-ray and neutron crystallography have provided molecular-level details of these different forms of crystalline cellulose and of their intracrystalline H-bonding patterns.[34−53]

The recalcitrance of cellulose I_β to degradation (via enzymatic or acid catalyzed routes) to glucose is a critical roadblock to biofuels production and is thought to be related to its unusually high thermal and mechanical stability. Recent experiments show that it is easier to degrade cellulose III_I than cellulose I_β. Cellulose III_I has enhanced enzymatic hydrolysis rates by up to 5-fold with respect to cellulose I_β.[54−57] One possible explanation for this difference can be given in terms of a rearrangement of the H-bonding network. Several experimental and theoretical studies have probed the stabilization of different cellulose forms.[28,34,36,37,39,40,45−52,58−69] These studies show that a redundancy in the H-bonding pattern and an interdependency of intramolecular and intermolecular H-bonds play a central role in determining the high stability of crystalline cellulose and its resistance to enzymatic hydrolysis.[48,65] However, it is clear that H-bonds alone cannot fully explain the structural stability and chemical properties of cellulose and that other forces, particularly those between the stacked sheets of cellulose chains, must also play an important role.

Although interactions between adjacent cellulose chains within a single layer of cellulose (intrasheet interactions) are generally stabilized by conventional OH···O type H-bonds,[39,46] interactions between different layers of cellulose (intersheet interactions) are typically stabilized by stacking forces. However, in cellulose III_I, conventional OH···O type H-bonds also contribute to intersheet interactions.[43] Quantifying intermolecular stabilizing forces responsible for stacking up cellulose sheets is not straightforward. Typically, stabilization due to stacking in cellulose originates from vdW forces, and these forces can marginally contribute to intrasheet interactions, as well.[59,66,67] Recently, intermolecular interactions among different allomorphs of cellulose have been compared on the basis of H-bonding geometries and crystal density.[52] Li et al. showed that vdW interactions contributed to both intersheet and intrasheet packing of two cellulose chains and that they played a role equally important as H-bonding in stabilizing the cellulose crystal structure.[69] X-ray and neutron diffraction studies indicate that nonconventional CH···O type H-bonding also contribute to both intrasheet[39,64] and intersheet interactions.[39,68]

In this study, we investigate properties of stacking interactions in cellulose I_β and III_I and their relative strength compared to H-bonds. We carry out systematic quantum chemical calculations on two small assemblies of cellulose I_β and cellulose III_I. Each assembly is composed of six cellobiose (dimeric fragment of glucose) units arranged in three layers (Figure 1) and is representative of the cellulose crystalline core not directly exposed to the aqueous environment. A detailed characterization and comparison of the H-bonding and stacking interactions in these assemblies provides new insights into the physical and chemical nature of the different crystalline cellulose allomorphs and their differential susceptibility to enzymatic or acid-catalyzed hydrolysis. We note that the reported stabilization energies due to H-bonding and stacking interactions include contributions from nonconventional CH···O type of H-bonds, as well. This effort serves as a first attempt to quantify the interplay between stacking and H-bonding in carbohydrates.

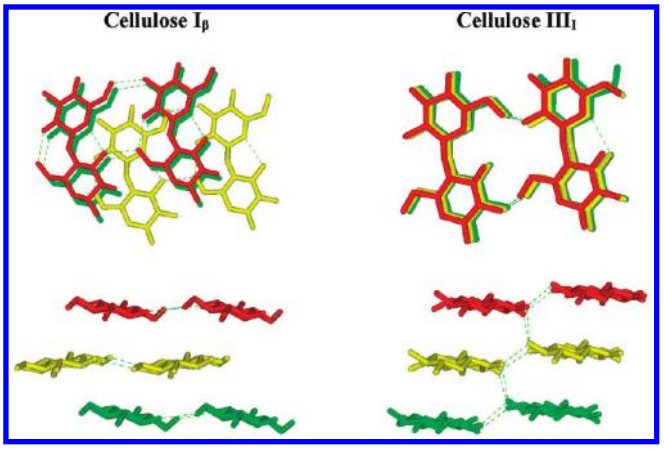

Figure 1. Side and top views of the central crystalline cores of the cellulose I_β and III_I considered in the quantum chemical study. Hydrogen atoms are not shown but are included in the calculations. Different colors mark different layers. Dotted lines are indicating the OH···O type of H- bonding contacts.

COMPUTATIONAL DETAILS

The configurations for our quantum chemical calculations correspond to representative structures of the central crystalline cores of both cellulose I_β and III_I fibrils. As shown in Figure 1, the crystalline core model system is composed of six cellobiose fragments arranged in three layers. The three layers are denoted as layers 1, 2 and 3 (Figures S1 and S2 of the Supporting Information). The two individual cellobiose units composing each layer are identified as 1a and 1b (layer 1), 2a and 2b (layer 2), and 3a and 3b (layer 3). These structures were generated from molecular dynamics (MD) simulations on water-solvated cellulose I_β and III_I model fibrils, each composed of 30 glucan chains (See Figure S3 in the Supporting Information). Detailed MD simulation methods used in this investigation are given as Supporting Information. We obtained average-representative structures by applying a single-linkage clustering algorithm to our equilibrated MD trajectories.[70] The maximum value for the root mean squared deviation (rmsd), calculated from the equilibrated MD trajectories, from these average structures was found to be ∼0.7 Å for both cellulose I_β and III_I.

MD-generated, rather than crystallographically determined, structures were used as starting points in our quantum chemical calculations for two main reasons. First, we wanted to consider structures that are representative of the relatively small cellulose fibrils (∼30 glucan chains) found in plant biomass, rather than the much larger cellulose nanocrystals from seaweeds and tunicates, which have been used in crystallographic analyses.[39] Second, we wanted to consider water-solvated structures at room temperature and pressure and, therefore, the effects of thermal noise. Although the MD simulations considered these cellulose fibers in explicit water, quantum chemical calculations were performed only on their smaller crystalline cores, which are composed of cellulose chains that are not directly exposed to the aqueous environment. This removes the need to directly consider the contributions of hydrophobic interactions, although they will be relevant when considering more complete systems

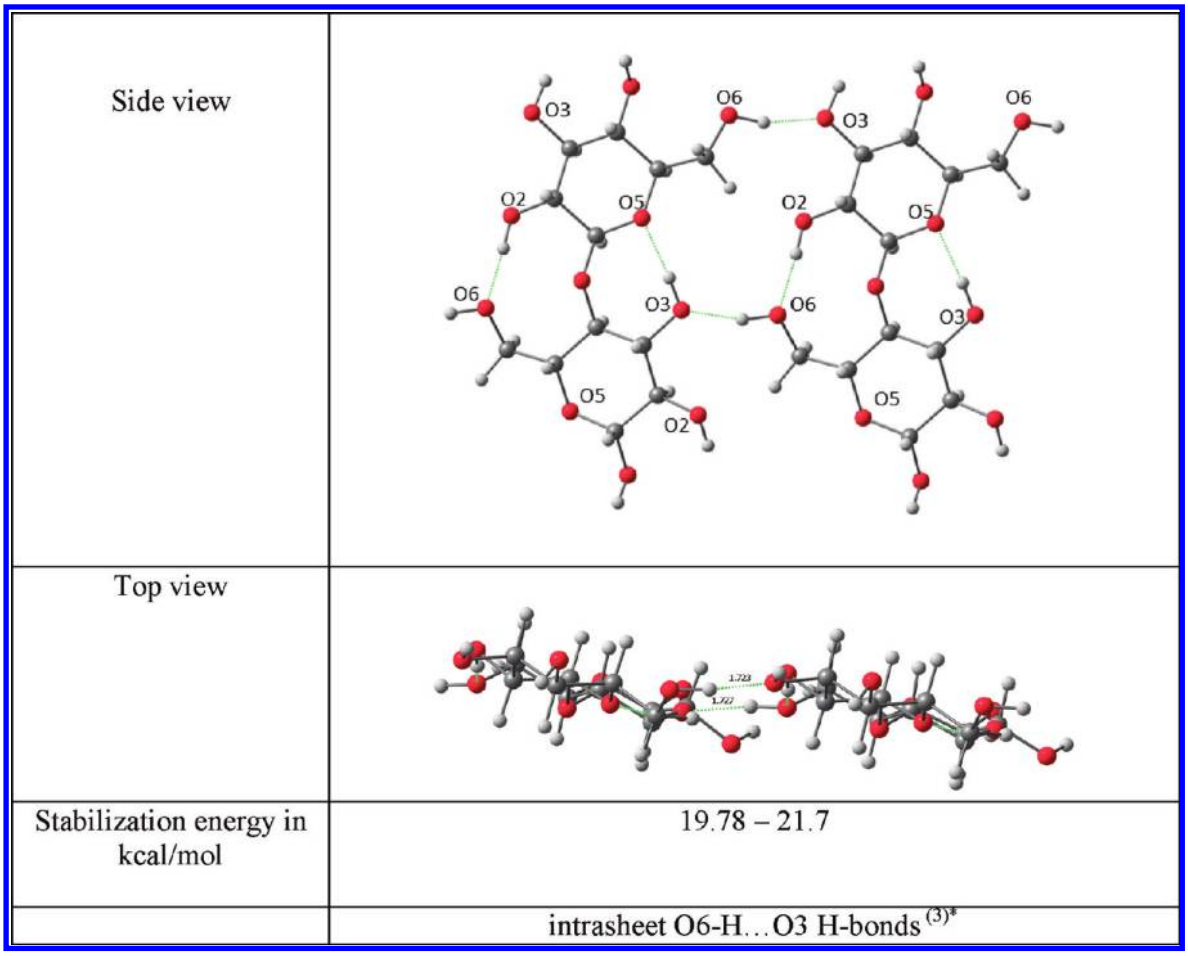

Figure 2. Intrasheet H-bonding pattern in cellulose I_β. The asterisk indicates the number of different subunits isolated from the overall assembly considered for the calculation of stabilization energies.

that include water or enzymes directly interacting with the surface cellulose chains.[33,59]

It is worth mentioning that the MD-generated structures of the cellulose I_β and III_I crystalline cores agree well with the experimental structures observed in X-ray and neutron diffraction studies.[39,43] This indicates that the propagation of surface effects to the crystalline core is minimal. Indeed, the calculated crystal unit parameters deviate from their experimental values by 3−8%. These deviations are expected for MD simulations performed at T = 298 K on a water-solvated cellulose fibril.[51] In more detail, the crystal unit parameters that are important in terms of noncovalent interactions are the ones in the plane orthogonal to the fibril main axis; namely, a and b.[46] These parameters are directly related to and defined by noncovalent interactions (dispersion interactions and H-bonds), respectively.[71] The relative deviations for a and b calculated for both cellulose I_β and III_I from MD simulations vary in the interval 1.2−4.8%.[57]

All quantum calculations were carried out using the Gaussian09 suite programs.[72] The newly developed hybrid meta density functional M06-2x from Truhlar's group[73] with 6-31+(d,p) was employed to calculate the stabilization energies using single point calculation on the selected cellulose assemblies and its subunits geometries. The functional M06-2x chosen for this study has been shown to provide a good level of description for nonbonded interactions, including H-bonds and stacking interactions in a wide variety of biomolecular complexes.[23,73−80] Calculations were carried out on all possible combinations of subunits of the crystalline cores varying from two to six cellobiose units (Figures S1 and S2 of the Supporting Information). The total stabilization energies (SEs) for both cellulose I_β and III_I assemblies and for each subunit were calculated as

$$\mathrm{SE} = -\left(E_{\mathrm{Complex}} - \sum_{i}^{n} E_i\right) \quad (1)$$

where E_{complex} is the total energy of the assembly/subunit used in the calculation, E_i is energy of the ith cellobiose unit and n is the total number of cellobiose units in the subunit/assembly.

The contributions from both intrasheet and intersheet H-bonding and intersheet stacking energies were decomposed from the total energy of the respective subunits/assembly to quantify their individual contributions to stabilization. The decomposition was carried out by predefining the type of interactions, either H-bonding or stacking, among these different subunits. For example, the interaction between 1a and 2a units (1a + 2a) is classified entirely as stacking interaction contributing to intersheet stability in both cellulose I_β and III_I. However, the interaction between 1a and 2b (1a + 2b) is classified as an intersheet stacking interaction in cellulose I_β and as an intersheet H-bonding interaction in cellulose III_I. This was based on the known structural and packing details of these crystalline forms. In cellulose I_β, both 2a and 2b in the second layer make stacking contacts with 1a. In cellulose III_I, 1a and

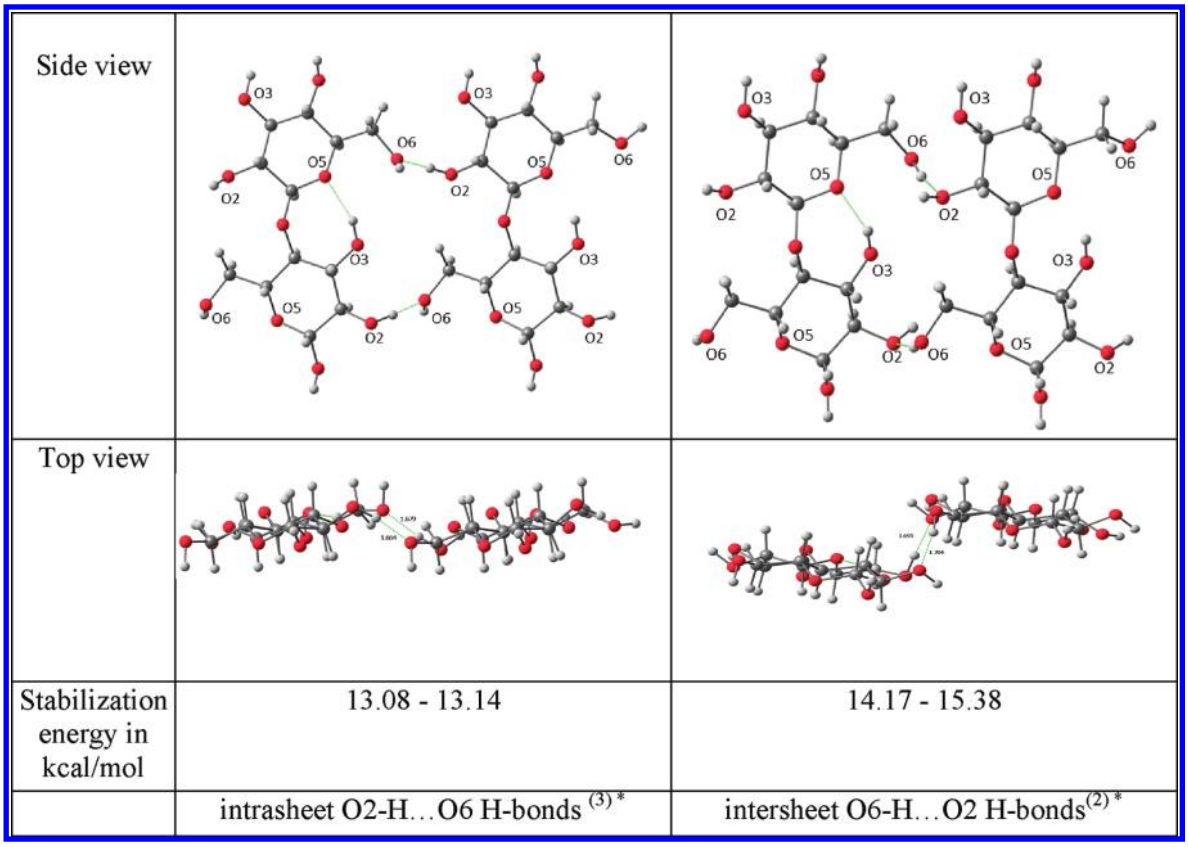

Figure 3. Intrasheet and intersheet H-bonding patterns in cellulose III_I. The asterisk indicates the number of different subunits isolated from the overall assembly considered for the calculation of stabilization energies.

2a units are almost aligned on top of each other. Therefore, stacking interactions originate primarily between 1a and 2a units.

Unlike in cellulose I_β, in cellulose III_I, unit 1a forms conventional H-bonds with the 2b unit (1a + 2b) that contributes toward intersheet H-bond interactions. Similar knowledge-based assignments were made for the other subunit interactions. We note that not all combinations of 2, 3, and 4 cellobiose units from the entire cellulose core crystalline model are symmetrically identical. In addition, initial MD-generated structures possess some degree of heterogeneity within symmetrically identical combinations. For these reasons, we observe slightly different energies for different combinations of cellobiose units and their range is reported. Additional details of our methodological approach and all different subunits considered in this study (Tables S1 and S2) have been provided as Supporting Information.

On the basis of the above definition, our clarification of H-bonding and stacking interactions does not rigorously follow the textbook description of those interactions. We clarify that the reported energies for intrasheet H-bonding are primarily from conventional OH···O type H-bonds but also include minor contributions from nonconventional CH···O type H-bonds and vdW forces, even though we do not explicitly quantify the contributions from such interactions. Similarly, intersheet interactions will contain contributions from vdW forces and CH···O interactions, and we do not explicitly report the contribution from these interactions to the total SEs of H-bonding and stacking. For example, some of the CH···O interactions will contribute to the calculated intersheet stacking, and it is also possible that intersheet H-bonding may have minor contribution from vdW interactions. The atoms-in-molecules (AIM)[81] approach was used in this investigation to confirm contributions from nonconventional CH···O type H-bonds. The AIM calculations were carried out using the AIM 2000 package.[82] The wave functions generated from the quantum chemical calculations using M06-2x/6-31+(d,p) were used to generate the electron density topography of cellulose I_β and cellulose III_I conformations.

RESULTS AND DISCUSSION

Intrasheet and Intersheet H-Bonding Interactions in Cellulose Models. In cellulose I_β, there are two types of intrachain (O2−H···O6 and O3−H···O5) H-bonds and one type of intrasheet O6−H···O3 (bifurcated to O3) H-bond between neighboring cellobiose units within a single sheet (Figure 2). The energies of the intrasheet H-bonds are in the range of 19.78−21.7 kcal/mol (per cellobiose pair). Conversely, cellulose III_I has one intrachain O3−H···O5 H-bond, one intrasheet O2−H···O6 H-bond, and one intersheet O6−H···O2 H-bond between neighboring cellobiose units (Figure 3). Mostly, this difference is facilitated by the rotation of the hydroxymethyl (O6) group away from its *tg* orientation in cellulose I_β to the *gt* orientation in cellulose III_I. The hydroxyl (O2) group also rotates from its corresponding orientation in cellulose III_I to its cellulose I_β orientation. The O2−H···O6 intrasheet H-bonding network has energies in the range of 13.08−13.14 kcal/mol, and the O6−H···O2 intersheet H-bonding network has energies in the range of 14.17 − 15.32 kcal/mol. Therefore, although there is only one type (O6−H···O3) of intrasheet H-bonding interaction in cellulose I_β, it is stronger than both types of intrasheet

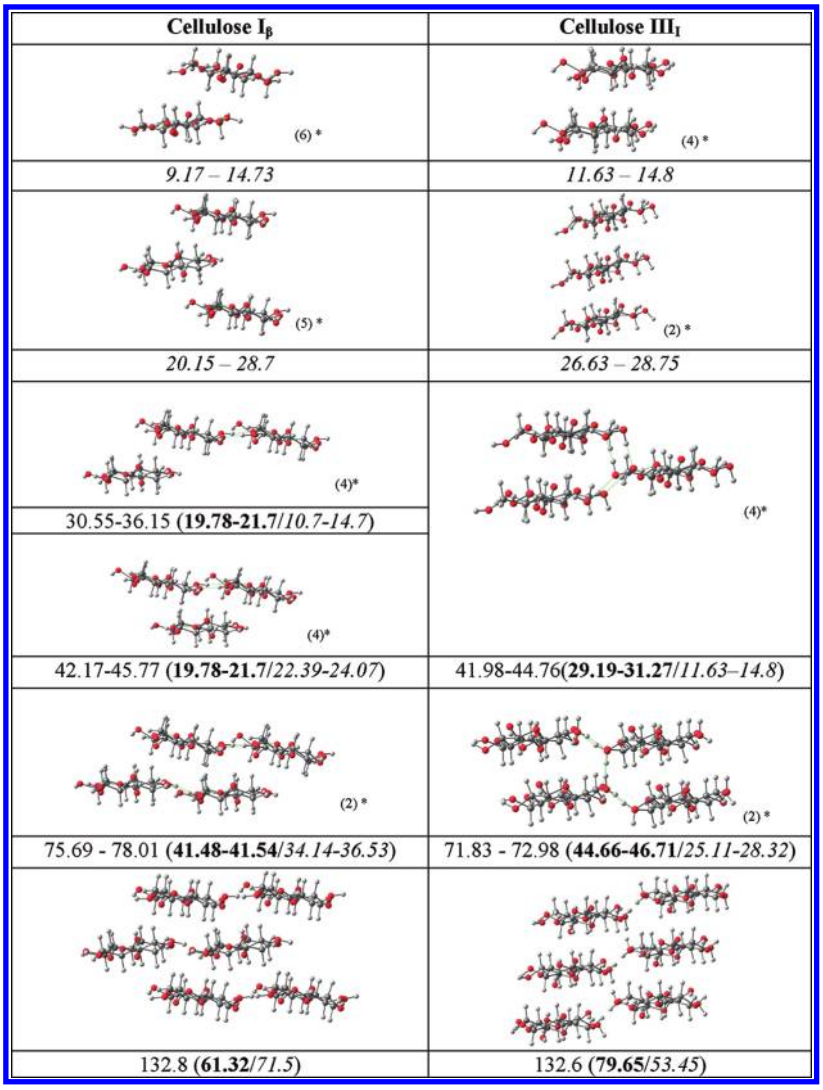

Figure 4. Intersheet stacking patterns in cellulose I_β and cellulose III_I. Stabilization energies in kcal/mol. Intrasheet H-bonding (bold) and intersheet stacking (italics) contributions are given in parentheses. An asterisk indicates the number of different subunits isolated from the overall assembly considered for the calculation of SE.

O2−H···O6 and intersheet O6−H···O2 H-bonds in cellulose III_I. Overall, the rearrangement of H-bonding in cellulose III_I results in more numerous but weaker H-bonding interactions among the cellobiose units.

Intersheet Stacking Interactions in Cellulose Models. Crystallographic structures reveal that stacking patterns are very different between cellulose I_β and III_I. In cellulose III_I, the glucose rings are stacked on top of each other, but in cellulose I_β, they partially overlap (see Figure 1). Stacking interactions were calculated in a step-by-step manner; that is, considering first two cellobiose units in two adjacent layers and then systematically adding cellobiose units to eventually obtain a three layer configuration with two chains per layer (Figure 4). In cellulose III_I, the stacking of two and three cellobiose units results in stabilization energies of 11.63−14.8 and 25.63−28.75 kcal/mol, respectively. In cellulose I_β, similar stacking of two and three units results in stabilization energies of 9.17−14.73 and 20.15−28.7 kcal/mol, respectively. Thus, in general, the stacking of cellobiose units in cellulose III_I core results in slightly higher or comparable individual stacking energy contributions compared with those observed in cellulose I_β. However, we observe that stabilization due to stacking interactions increases drastically in cellulose I_β when the number of stacked cellobiose units is gradually increased (see below). This can be rationalized in terms of the packing in cellulose I_β, in which the numbers of stacking contacts are favorably enhanced upon addition of cellobiose units with respect to cellulose III_I.

Cooperative Nature of Intermolecular Forces in Cellulose Models. To investigate the cooperative nature of H-bonding in both cellulose I_β and III_I allomorphs, we consider the H-bonding energetic contributions in different subunits of the starting crystalline core (see Figures S1 and S2 of the Supporting Information) normalized over the number of cellobiose units present in each subunit. Cooperativity in the H-bond network is estimated from a linear fit of the normalized stabilization energies (Figure 5A). Positive and negative values for the slope (a) indicate positive and negative cooperativity, respectively, whereas a slope $a = 0$ indicates additivity, that is, negligible cooperativity. In cellulose I_β, $a = 0.02 \pm 0.1$ ($R^2 = 0.83$) is consistent

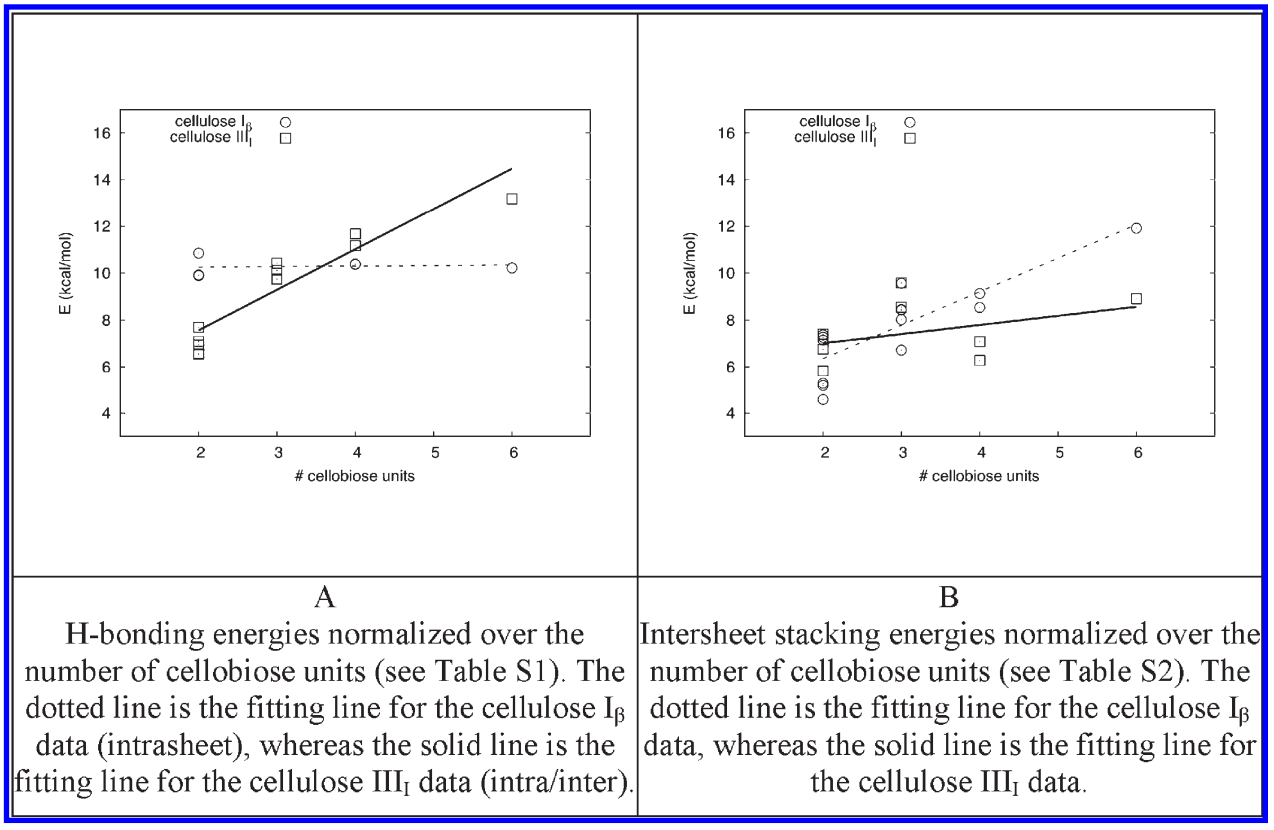

Figure 5. Contributions from (A) H-bonding and (B) intersheet stacking interactions to the stabilization as a function of number of cellobiose units.

with an additive intrasheet H-bond formation mechanism. For cellulose III_I, $a = 1.73 \pm 0.02$ ($R^2 = 0.87$) consistent with positive cooperativity in H-bond interactions. Within the set of structures analyzed in this study, individual H-bonds appear to be stronger in cellulose I_β than in cellulose III_I, whereas H-bonding cooperative effects are observed in cellulose III_I. The cooperative nature of H-bonding in cellulose III_I leads to a larger total contribution of H-bonding to the stabilization in cellulose III_I[52] in comparison with cellulose I_β. Extended zigzag networks of homodromic ···O2−H···O6−H···O2··· H-bonds were identified in the crystallographic studies of cellulose III_I as being potentially cooperative and contributing to the metastability of this crystalline form.[43,52] We note that earlier theoretical studies reporting on the cooperative nature of H-bonding in cellulose considered a single cellulose chain and, therefore, only that of intrachain H-bonding,[63] but the current study focuses on interchain H-bonding in the presence of multiple sheets.

The cooperativity in stacking interactions has been quantified by linearly fitting the stacking energy values normalized over the number of cellobiose units. Figure 5B shows that intersheet stacking interactions are highly cooperative in cellulose I_β, where the slope of the fitting line is $a = 1.43 \pm 0.26$ ($R^2 = 0.88$), and weakly cooperative in cellulose III_I, where $a = 0.39 \pm 0.32$ ($R^2 = 0.85$). The largest cellulose assembly considered in our calculations is composed of six cellobiose units in three layers. The overall stabilization energy for this assembly of cellulose I_β and cellulose III_I is 132.8 and 132.6 kcal/mol, respectively. In cellulose I_β, stacking interactions (71.5 kcal/mol) contribute a little more than H-bonding (61.32 kcal/mol), 54% and 46%, respectively. On the other hand, in cellulose III_I, the contributions from H-bonds (79.15 kcal/mol) give a larger contribution to stabilization than stacking interactions (53.45 kcal/mol), 60% and 40%, respectively. Hence, it is likely that the high stability reported[53−57] for cellulose I_β originates from both strong intrasheet H-bonding interactions and highly cooperative intersheet stacking interactions.

Effect of Basis Set Superposition Error (BSSE) on the Stabilization of Cellulose Models. Stabilization energies were calculated at the M06-2x/6-31+(d,p) level using the supermolecule approach and corrected for BSSE following the counterpoise procedure adopted by Boys and Bernardi[83] for the selected two cellobiose units. Evaluation of BSSE correction is necessary when calculating the stabilization energies of nonbonded complexes. We carried out stabilization energy calculations with BSSE correction for complexes composed of two cellobiose units in both intrasheet/intersheet H-bonding (Figures 2 and 3) and intersheet stacking conformations (see top column of Figure 4). In cellulose I_β, average BSSE corrected energies for intrasheet H-bonding and intersheet stacking are 18.4 and 9.2 kcal/mol, respectively (Table S1 in Supporting Information). The corresponding deviations from the BSSE uncorrected stabilization energies are 2.03 ± 0.05 kcal/mol and 3.06 ± 0.5 kcal/mol for intrasheet H-bonding and intersheet stacking, respectively.

In cellulose III_I, the average BSSE-corrected energies for intrasheet/intersheet H-bonding and intersheet stacking are 11.7 and 8.8 kcal/mol (Table S2 in the Supporting Information). The corresponding deviations from the BSSE-uncorrected stabilization energies are 2.25 ± 0.2 and 4.5 ± 0.03 kcal/mol for intrasheet/intersheet H-bonding and intersheet stacking, respectively. Stacking energies exhibit slightly larger deviation than the

Table 1. Electron Density ($\rho(r_c)$) and Laplacian of Electron Density ($\nabla^2\rho(r_c)$) for Intermolecular Interactions in Cellulose I_β and III_I

Cellulose I_β	Intrasheet Interactions	$\rho(r_c)$, e/a_0^3	$\nabla^2\rho(r_c)$, e/a_0^5	Intrasheet Interactions	$\rho(r_c)$, e/a_0^3	$\nabla^2\rho(r_c)$, e/a_0^5
layer 1: 1a+1b	O6−H···O3	0.038	0.035	C−H···O2	0.008	0.007
	O3···H−O6	0.038	0.034	O2···H−C	0.007	0.006
layer 2: 2a+2b	O6−H···O3	0.031	0.026	C−H···O2	0.006	0.003
	O3···H−O6	0.032	0.026	O2···H−C	0.005	0.003
layer 3: 3a+3b	O6−H···O3	0.04	0.037	C−H···O2	0.008	0.006
	O3···H−O6	0.038	0.034	O2···H−C	0.008	0.007
Cellulose III_I	Intrasheet interactions	$\rho(r_c)$, e/a_0^3	$\nabla^2\rho(r_c)$, e/a_0^5	Intrasheet interactions	$\rho(r_c)$, e/a_0^3	$\nabla^2\rho(r_c)$, e/a_0^5
layer 1: 1a + 1b	O6···H−O2	0.043	0.038	C−H···O3	0.003	0.003
	O2−H···O6	0.044	0.039	O6···O3	0.005	0.005
layer 2: 2a + 2b	O6···H−O2	0.044	0.039	C−H···O3	0.003	0.003
	O2−H···O6	0.046	0.04	O3···O6	0.004	0.005
layer 3: 3a + 3b	O6···H−O2	0.041	0.036			
	O2−H···O6	0.042	0.036			
	Intersheet Interactions			Intersheet Interactions		
1a + 2b	O6−H···O2	0.043	0.037	C−H···O3	0.004	0.004
	O2···H−O6	0.043	0.036	O6···H−C	0.005	0.005
				O3···H−C	0.005	0.005
				C−H···O6	0.007	0.006
2b + 3a	O6−H···O2	0.042	0.035	C−H···O3	0.006	0.005
	O2···H−O6	0.044	0.038	O6···H−C	0.006	0.006
				O3···H−C	0.003	0.002

H-bonding energies for the selected model systems. We expect the relative differences between uncorrected and BSSE-corrected energies to remain similar in the larger assemblies.[84] Hence, BSSE-uncorrected energies were considered for general comparison.

Characterization of Intermolecular Forces of Cellulose Using AIM Theory. The atoms-in-molecules (AIM) theory offers a rigorous way to partition any molecular system into atomic fragments by considering the gradient vector field of its electron density.[81] Topological features such as bond critical points (BCP) and paths of maximum electron density can be utilized to draw molecular graphs. It has been shown in previous reports[21,25,81,85−101] that the AIM theory provides clear information about the predominant and secondary interactions involved in the stabilization of intermolecular complexes. The AIM theory has been successfully applied to characterize covalent, noncovalent, and conventional/improper H-bonding and stacking interactions in a variety of molecular systems.[21,25,81,85−101]

The calculated electron density and its Laplacian at the BCP for H-bonding interactions of cellulose I_β (intrasheet) and cellulose III_I (intra-/intersheet) are listed in Table 1. The calculated electron density values for the OH···O (10^{-2} au), CH···O (10^{-3} au), and O···O (10^{-3} au) interactions are in accordance with the standards reported for these interactions.[95] Positive values of the Laplacian of the electron density also follow a similar trend.[95] The electron density topology of the molecular graphs along with the bond paths of intrasheet/intersheet H-bonding and intersheet stacking arrangements are shown in Figures 6 and 7 for cellulose I_β and III_I, respectively. The existence of conventional OH···O H-bonds between intermolecular complexes is demonstrated by the presence of the bond critical points. Apart from identifying the conventional H-bonding, the presence of BCPs and bond paths also identify CH···O and O···O interactions between cellobiose units.

Contribution from Nonconventional CH···O Type H-Bonding in Cellulose Models. In our description, nonconventional CH···O type H-bonding can contribute to both H-bonding and stacking interactions. In Figures 6 and 7, we have also provided the number of CH···O interactions identified from AIM analyses. It is interesting to note that electron density analysis clearly portrays the relative importance of these nonconventional H-bonded interactions in the stabilization of intra/intersheet arrangements. In cellulose I_β, there are two weak CH···O H-bonds between the cellobiose units. This gives rise to H···O distances (2.6 Å) that are considerably shorter than the sum of the normal vdW radii (2.72 Å) of the hydrogen (1.2 Å) and oxygen atoms (1.52 Å).[52] In addition, cellulose III_I has more intersheet CH···O type interactions than cellulose I_β.

The $\rho(r_c)$ values at the BCPs corresponding to the CH···O interactions (10^{-3} au) are lower than those corresponding to OH···O H-bonding interactions (10^{-2} au). The molecular topology of intersheet stacking interactions between cellobiose units (Figures 6 and 7) indicates, in addition to vdW and nonpolar CH···C interactions, multiple CH···O interactions also provide non-negligible contribution to stacking interactions.

Molecular Electrostatic Potential of Cellulose Models. The molecular electrostatic potential (MESP) can be used to explore the reactivity of a molecular system.[102] It identifies regions of electron localization in the molecule and therefore the probable sites of electrophilic or nucleophilic attack. The MESP maps for cellulose I_β and III_I are shown in Figure 8. Structures with the same orientation are shown side-by-side the MESP surface for

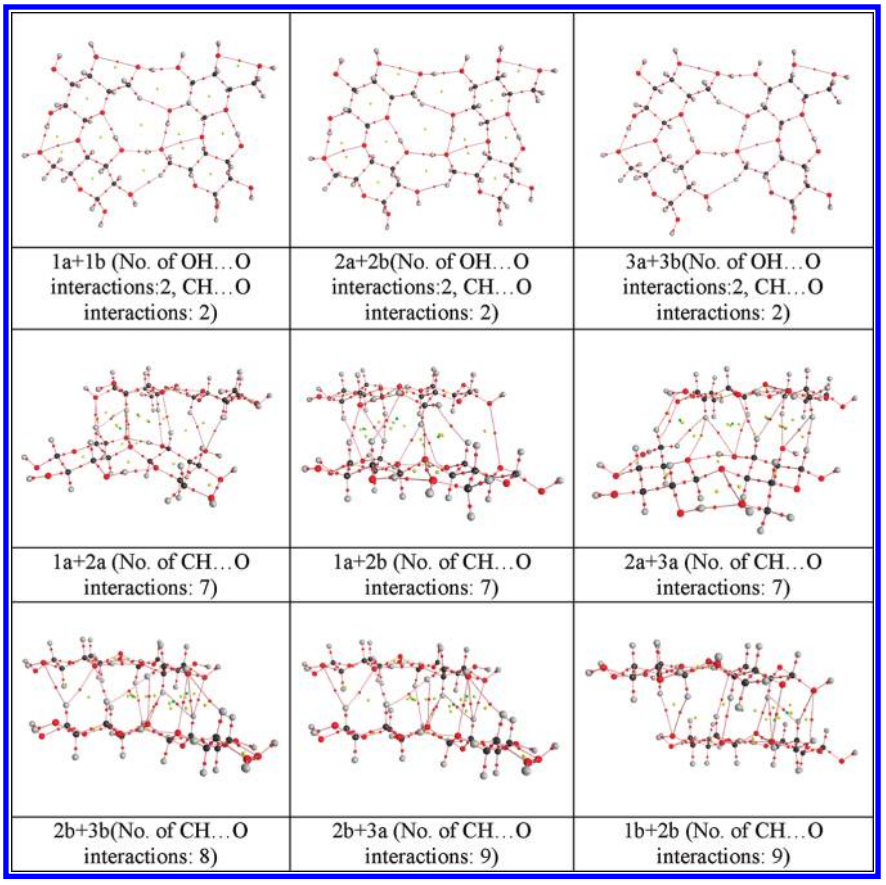

Figure 6. Molecular graphs of intra/intersheet interactions in cellobiose complex for cellulose I_β.

better identification of the reactive sites (Figure S4 of the Supporting Information). We expect to observe similar MESP for (1,0,0) and (−1,0,0) surfaces based on the crystalline symmetry of cellulose I_β,. However, the expected symmetry in MESP is perturbed by the fact that we consider a truncated smaller fragment of a cellulose fibril made up of three layers where boundary conditions strongly influence the observed MESP. Hence, we carried out separate MESP analysis on the first (1,0,0) and the third (−1,0,0) layer of cellulose I_β without considering the middle layer. The results of these additional MESP analysis of a layer are reported in the Supporting Information (Figure S5) and show an improved symmetry in the MESP between (1,0,0) and (−1,0,0) surfaces.

In cellulose I_β, donor and acceptor atoms are only partially exposed. Conversely, in cellulose III_I, most of the donor and acceptor atoms are favorably exposed. The regions associated with the lone pairs of the oxygen atoms provide possible anchoring sites for further H-bonding interactions. Alternate red and blue regions in cellulose III_I show that this is a preferred system for interaction with water molecules and polar amino acid residues in the cellulose binding modules (CBM) or catalytic active site of cellulases. Thus, MESP indicates the preferred solvation and reactivity of cellulose III_I compared with cellulose I_β.

Furthermore, nonpolar regions are more accessible in cellulose I_β surfaces than in cellulose III_I. Both (1,0,0) and (−1,0,0) surfaces exhibit neutral regions in cellulose I_β, whereas in cellulose III_I, distinct accumulation of positive and negative potential is clearly seen (Figure 8). We considered additional types of cross sections of the elementary cellulose I_β fibril models[60,61,103] (Figure S6 of the Supporting Information), and the results are provided in the Supporting Information. The other views of MESP (Figure S7 of the Supporting Information) show that the faces of cellulose I_β fibril such as (1,−1,0), (−1,−1,0), (1,1,0), and (−1,1,0) are mostly stabilized by stacking forces. Interestingly, (1,1,0) and (−1,1,0) surfaces exhibit a uniformly distributed, positively charged region.

Enzymatic Digestibility of Crystalline Cellulose. Our findings provide several new insights that are relevant to recent experiments that show differences in enzyme digestibility rates between cellulose I_β and III_I. Those experiments clearly show enhanced hydrolysis rates for cellulose III_I, by up to 5-fold with respect to cellulose I_β.[54,56,57] However, the binding affinities of the cellulases (all containing family 1 CBMs) to cellulose I_β were higher than those observed in cellulose III_I. These somewhat conflicting observations can be explained in terms of the differences arising from the cellulose structural arrangements and the interplay of H-bonding and stacking interactions, as discussed above. In cellulose I_β, the homogeneous exposure of a large number of nonpolar groups on (1,0,0) and (−1,0,0) surfaces and the cooperative stacking interactions may contribute to enhance the hydrophobic nature of the surface, which can explain the enhanced binding affinities of carbohydrate binding domains of cellulases. Indeed, binding of CBM's to cellulose I_β is thought to arise largely from hydrophobic interactions between the three planar aligned aromatic residues in the CBM and the cellulose surface.[104]

In cellulose III_I, however, the "tilted" arrangement of the glucose rings (See Figure 1) makes both polar and nonpolar

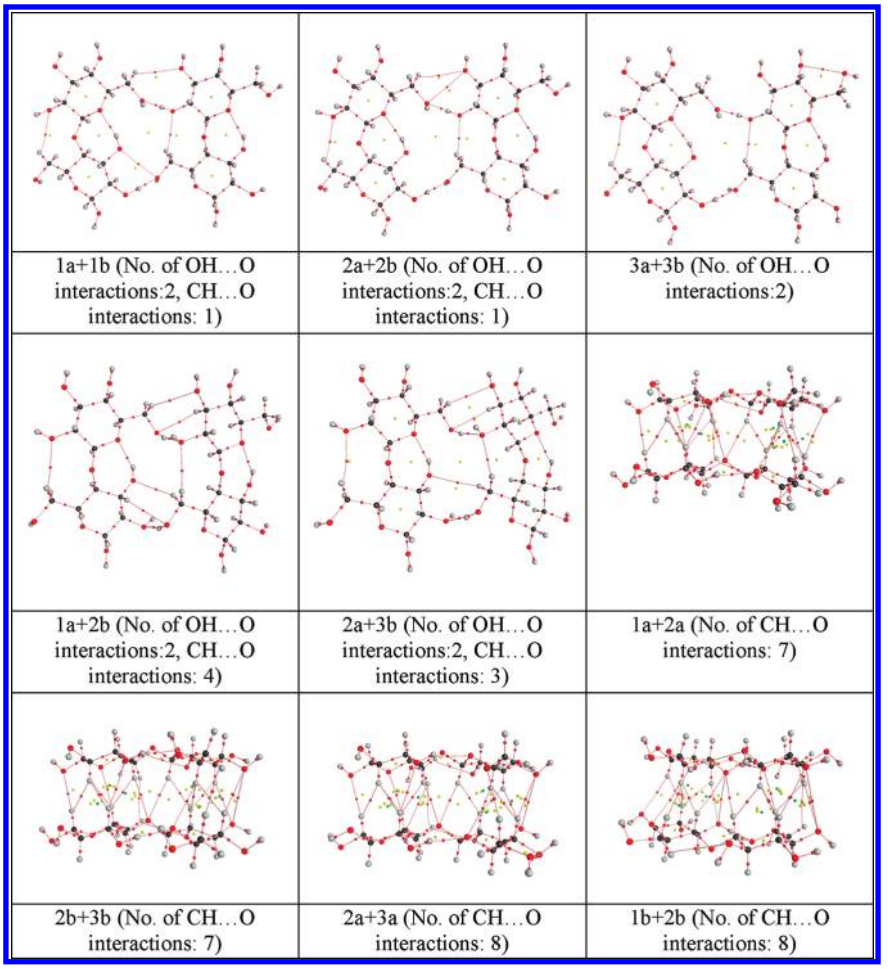

Figure 7. Molecular graphs of intra/intersheet interactions in cellobiose complex for cellulose III_I.

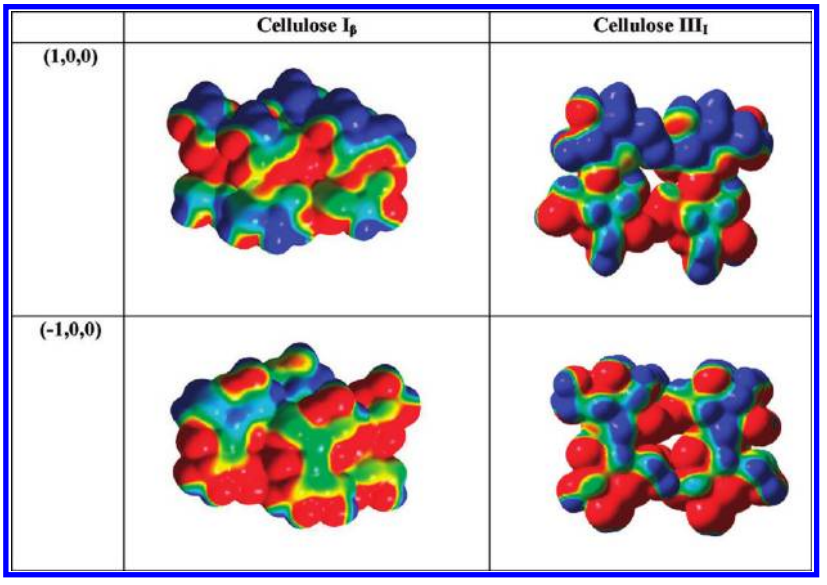

Figure 8. Molecular electrostatic potential map of cellulose I_β and cellulose III_I at the ±0.04 au isosurface. The color scale indicates the charges on the atoms: red = most negative, green = neutral, blue = most positive charge. Structures with the same orientation are shown side-by-side the MESP surface for better identification of the reactive sites as Supporting Information.

components easily accessible on surfaces. This allows cellulose III_I to take part in more specific interactions with bulk water and enzymes. Recent work has implicated several polar amino acid residues in the binding/processivity of family 1 CBMs on

cellulose,[105] which could likely play a more important role for cellulose III_I.[54,57] In addition, the favorable exposure of the glycosidic oxygens on the (1,0,0) surface of cellulose III_I might help explain its enhanced hydrolysis rates. The possible interactions of the hydroxyl groups of cellulose III_I are also responsible for the first-order kinetic behavior reported for hydroxyl groups reacting with various chemicals (e.g., silylating or carboxymethylating agents) that is reminiscent of homogeneous phase reactions, although it is a heterogeneous reaction system.[106,107] These results suggest that the improved accessibility of the hydroxyl groups and glycosidic oxygens in cellulose III_I is responsible for its enhanced reactivity compared with native cellulose I_β.

CONCLUSIONS

We present the results of quantum chemical calculations aimed at quantifying the energy contributions of H-bonding and stacking interactions to the stabilization of crystalline cores of solvated cellulose I_β and III_I fibrils. We observe that both types of noncovalent interactions are contributing equally to the stabilization of cellulose crystalline structures. In addition, the atoms-in-molecules theory is used to provide evidence of CH···O interactions contributing to both intrasheet and intersheet stabilization. Specific details of these interactions are utilized to infer the connection between the substrate chemical properties of the cellulose III crystalline core and its enhanced reactivity to enzymes/chemicals. Our calculations also reveal that both H-bonds and stacking interactions can exhibit cooperative behavior. In the naturally occurring cellulose I_β, strong cooperative stacking interactions contribute to its structural stability slightly more than H-bonds. Thus, both interactions need to be taken into account when designing novel chemical pretreatment protocols (e.g., ionic liquids) and enzymes for improved catalysis of cellulosic biomass for biofuel production.

We also note in passing that the long-standing discussion of crystallinity as a key contributing factor to the recalcitrance of cellulosic biomass must now become much more sophisticated. On the basis of our results, it is inadequate to simple refer to cellulose as "crystalline" or "amorphous". Both cellulose I_β and cellulose III_I are crystalline assemblages of cellobiose units. However, the nature of the H-bonding and stacking of chains profoundly influences the access of water, enzymes, and chemicals to exposed crystal faces, as we have shown by experiments and now clearly confirmed by theoretical calculations.

ASSOCIATED CONTENT

Supporting Information. Description of the H-bonding and stacking arrangements of cellulose models, systematic calculations of the entire assembly and individual subunits, complete reference 72, details of methodology, and results are provided as Supporting Information. This material is available free of charge via the Internet at http://pubs.acs.org

AUTHOR INFORMATION

Corresponding Author

*Phone: 505-665-1923. Fax: 505-665-3493. E-mail: gnana@lanl.gov

ACKNOWLEDGMENT

This work is supported by LANL LDRD and NABC. R.P. acknowledges LANL Directors Postdoctoral program for the financial support. G.B. acknowledges CNLS for partial support. S.P.S.C. and B.E.D. thank the DOE Great Lakes Bioenergy Research Center (DOE BER Office of Science DE-FC02-07ER64494) for support. The authors gratefully acknowledge Dr. V. Subramanian, CLRI, for his generous help in AIM analysis. The authors thank Ms. Donna Fertig, Sly Fox Studio, for her art work in cover illustration.

REFERENCES

(1) Lehn, J. M. *Angew. Chem., Int. Ed. Engl.* **1988**, *27*, 89–112.
(2) Muller-Dethlefs, K.; Hobza, P. *Chem. Rev.* **2000**, *100*, 143–167.
(3) Riley, K. E.; Pitonak, M.; Jurecka, P.; Hobza, P. *Chem. Rev.* **2010**, *110*, 5023–5063.
(4) *Hydrogen Bonding — New Insights*; Grabowski, S. J., Ed.; In Challenges and Advances in Computational Chemistry and Physics; Leszczynski, J., Ed.; Springer: New York, 2006.
(5) Cerny, J.; Hobza, P. *Phys. Chem. Chem. Phys.* **2007**, *9*, 5291–5303.
(6) Elstner, M.; Hobza, P.; Frauenheim, T.; Suhai, S.; Kaxiras, E. *J. Chem. Phys.* **2001**, *114*, 5149–5155.
(7) Hobza, P. *Phys. Chem. Chem. Phys.* **2008**, *10*, 2581–2583.
(8) Hobza, P.; Sponer, J. *Chem. Rev.* **1999**, *99*, 3247–3276.
(9) Sponer, J.; Leszczynski, J.; Hobza, P. *J. Biomol. Struct. Dyn.* **1996**, *14*, 117–135.
(10) Vondrasek, J.; Kubar, T.; Jenney, F. E.; Adams, M. W. W.; Kozisek, M.; Cerny, J.; Sklenar, V.; Hobza, P. *Chem.—Eur. J.* **2007**, *13*, 9022–9027.
(11) Alhambra, C.; Luque, F. J.; Gago, F.; Orozco, M. *J. Phys. Chem. B* **1997**, *101*, 3846–3853.
(12) Perez, A.; Sponer, J.; Jurecka, P.; Hobza, P.; Luque, F. J.; Orozco, M. *Chem.—Eur. J.* **2005**, *11*, 5062–5066.
(13) Sponer, J.; Jurecka, P.; Marchan, I.; Luque, F. J.; Orozco, M.; Hobza, P. *Chem.—Eur. J.* **2006**, *12*, 2854–2865.
(14) Hobza, P.; Sponer, J. *J. Am. Chem. Soc.* **2002**, *124*, 11802–11808.
(15) Reha, D.; Kabelac, M.; Ryjacek, F.; Sponer, J.; Sponer, J. E.; Elstner, M.; Suhai, S.; Hobza, P. *J. Am. Chem. Soc.* **2002**, *124*, 3366–3376.
(16) Sponer, J.; Leszczynski, J.; Hobza, P. *J. Phys. Chem.* **1996**, *100*, 5590–5596.
(17) Sponer, J.; Leszczynski, J.; Hobza, P. *Biopolymers* **2001**, *61*, 3–31.
(18) Sponer, J.; Leszczynski, J.; Hobza, P. *THEOCHEM: J. Mol. Struct.* **2001**, *573*, 43–53.
(19) Sponer, J.; Riley, K. E.; Hobza, P. *Phys. Chem. Chem. Phys.* **2008**, *10*, 2595–2610.
(20) Svozil, D.; Hobza, P.; Sponer, J. *J. Phys. Chem. B* **2010**, *114*, 1191–1203.
(21) Parthasarathi, R.; Subramanian, V. *Struct. Chem.* **2005**, *16*, 243–255.
(22) Antony, J.; Grimme, S. *Phys. Chem. Chem. Phys.* **2008**, *10*, 2722–2729.
(23) Gu, J.; Wang, J.; Leszczynski, J.; Xie, Y.; Schaefer Iii, H. F. *Chem. Phys. Lett.* **2008**, *459*, 164–166.
(24) Parthasarathi, R.; Subramanian, V.; Sathyamurthy, N. *J. Phys. Chem. A* **2005**, *109*, 843–850.
(25) Parthasarathi, R.; Subramanian, V.; Sathyamurthy, N.; Leszczynski, J. *J. Phys. Chem. A* **2007**, *111*, 2–5.
(26) Bendova, L.; Jurecka, P.; Hobza, P.; Vondrasek, J. *J. Phys. Chem. B* **2007**, *111*, 9975–9979.
(27) Lee, E. C.; Kim, D.; Jurecka, P.; Tarakeshwar, P.; Hobza, P.; Kim, K. S. *J. Phys. Chem. A* **2007**, *111*, 3446–3457.
(28) Mohamed, M. N. A.; Watts, H. D.; Guo, J.; Catchmark, J. M.; Kubicki, J. D. *Carbohydr. Res.* **2010**, *345*, 1741–1751.
(29) Pitonak, M.; Neogrady, P.; Rezac, J.; Jurecka, P.; Urban, M.; Hobza, P. *J. Chem. Theory Comput.* **2008**, *4*, 1829–1834.

(30) Kumar, R. M.; Elango, M.; Subramanian, V. *J. Phys. Chem. A* **2010**, *114*, 4313–4324.
(31) Lucas, R.; Gómez-Pinto, I.; Aviñó, A.; Reina, J. J.; Eritja, R. n.; González, C.; Morales, J. C. *J. Am. Chem. Soc.* **2011**, *133*, 1909–1916.
(32) Davis, A. P.; Wareham, R. S. *Angew. Chem., Int. Ed.* **1999**, *38*, 2978–2996.
(33) Jarvis, M. *Nature* **2003**, *426*, 611–612. Frey-Wyssling, A. *Biochim. Biophys. Acta* **1955**, *18*, 166. Warwicker, J. O.; Wright, A. C. *J. Appl. Polym. Sci.* **1967**, *11*, 659.
(34) Langan, P.; Nishiyama, Y.; Chanzy, H. *J. Am. Chem. Soc.* **1999**, *121*, 9940–9946.
(35) Nishiyama, Y.; Okano, T.; Langan, P.; Chanzy, H. *Int. J. Biol. Macromol.* **1999**, *26*, 279–283.
(36) Langan, P.; Nishiyama, Y.; Wada, M.; Sugiyama, J.; Chanzy, H. *Abstr. Pap. Am. Chem. Soc.* **2000**, *219*, 34-CELL.
(37) Langan, P.; Nishiyama, Y.; Chanzy, H. *Biomacromolecules* **2001**, *2*, 410–416.
(38) Nishiyama, Y.; Chanzy, H.; Langan, P. *Abstr. Pap. Am. Chem. Soc.* **2002**, *223*, 294-POLY.
(39) Nishiyama, Y.; Langan, P.; Chanzy, H. *J. Am. Chem. Soc.* **2002**, *124*, 9074–9082.
(40) Nishiyama, Y.; Chanzy, H.; Wada, M.; Sugiyama, J.; Langan, P. *Abstr. Pap. Am. Chem. Soc.* **2003**, *225*, 37-CELL.
(41) Nishiyama, Y.; Kim, U. J.; Kim, D. Y.; Katsumata, K. S.; May, R. P.; Langan, P. *Biomacromolecules* **2003**, *4*, 1013–1017.
(42) Nishiyama, Y.; Sugiyama, J.; Chanzy, H.; Langan, P. *J. Am. Chem. Soc.* **2003**, *125*, 14300–14306.
(43) Wada, M.; Chanzy, H.; Nishiyama, Y.; Langan, P. *Macromolecules* **2004**, *37*, 8548–8555.
(44) Langan, P.; Sukumar, N.; Nishiyama, Y.; Chanzy, H. *Cellulose* **2005**, *12*, 551–562.
(45) Wada, M.; Nishiyama, Y.; Langan, P. *Macromolecules* **2006**, *39*, 2947–2952.
(46) Nishiyama, Y.; Johnson, G. P.; French, A. D.; Forsyth, V. T.; Langan, P. *Biomacromolecules* **2008**, *9*, 3133–3140.
(47) Wada, M.; Nishiyama, Y.; Chanzy, H.; Forsyth, T.; Langan, P. *Powder Diffr.* **2008**, *23*, 92–95.
(48) Shen, T. Y.; Langan, P.; French, A. D.; Johnson, G. P.; Gnanakaran, S. *J. Am. Chem. Soc.* **2009**, *131*, 14786–14794.
(49) Wada, M.; Heux, L.; Nishiyama, Y.; Langan, P. *Cellulose* **2009**, *16*, 943–957.
(50) Wada, M.; Heux, L.; Nishiyama, Y.; Langan, P. *Biomacromolecules* **2009**, *10*, 302–309.
(51) Bellesia, G.; Asztalos, A.; Shen, T. Y.; Langan, P.; Redondo, A.; Gnanakaran, S. *Acta Crystallogr., Sect. D: Biol. Crystallogr.* **2010**, *66*, 1184–1188.
(52) Nishiyama, Y.; Langan, P.; Wada, M.; Forsyth, V. T. *Acta Crystallogr., Sect. D: Biol. Crystallogr.* **2010**, *66*, 1172–1177.
(53) Nishiyama, Y.; Wada, M.; Hanson, B. L.; Langan, P. *Cellulose* **2010**, *17*, 735–745.
(54) Chundawat, S. P. S.; Beckham, G. T.; Himmel, M. E.; Dale, B. E. *Ann. Rev. Chem. Biomol. Eng.* **2011**, *2*, 121–145.
(55) Chundawat, S. *Ultrastructural and physicochemical modifications within ammonia treated lignocellulosic cell walls and their influence on enzymatic digestibility*; Ph.D. Dissertation AAT 3417644, Michigan State University, East Lansing, 2009.
(56) Igarashi, K.; Wada, M.; Samejima, M. *FEBS J.* **2007**, *274*, 1785–1792.
(57) Chundawat, S. P. S.; Bellesia, G.; Uppugundla, N.; Sousa, L.; Gao, D; Cheh, A.; Agarwal, U. P.; Bianchetti, C. M.; Phillips, G. N., Jr.; Langan, P.; Balan, V.; Gnanakaran, S.; Dale, B. E. *J. Am. Chem. Soc.* **2011**, *133*, 11163–11174.
(58) French, A. D.; Johnson, G. P. *Cellulose* **2004**, *11*, 449–462. Ford, Z. M.; Stevens, E. D.; Johnson, G. P.; French, A. D. *Carbohydr. Res.* **2005**, *340*, 827–833. French, A. D.; Johnson, G. P. *Can. J. Chem., Rev. Can. Chim.* **2006**, *84*, 603–612.
(59) Nishiyama, Y.; Kuga, S.; Okano, T. *J. Wood Sci.* **2000**, *46*, 452.
(60) Qian, X. H.; Ding, S. Y.; Nimlos, M. R.; Johnson, D. K.; Himmel, M. E. *Macromolecules* **2005**, *38*, 10580–10589.
(61) Ding, S. Y.; Himmel, M. E. *J. Agric. Food Chem.* **2006**, *54*, 597–606.
(62) Bučko, T. s.; Tunega, D.; Ángyán, J. n. G.; Hafner, J. r. *J. Phys. Chem. A* **2011**, *115*, 10097.
(63) Qian, X. H. *Mol. Simul.* **2008**, *34*, 183–191.
(64) Yoneda, Y.; Mereiter, K.; Jaeger, C.; Brecker, L.; Kosma, P.; Rosenau, T.; French, A. *J. Am. Chem. Soc.* **2008**, *130*, 16678–16690.
(65) Shen, T. Y.; Gnanakaran, S. *Biophys. J.* **2009**, *96*, 3032–3040.
(66) Cousins, S. K.; Brown, R. M. *Polymer* **1995**, *36*, 3885–3888.
(67) Manjunath, B. R.; Venkataraman, A. *J. Polym. Sci.: Polym. Chem. Ed.* **1980**, *18*, 1407–1424.
(68) Bergenstråhle, M.; Berglund, L. A.; Mazeau, K. *J. Phys. Chem. B* **2007**, *111*, 9138–9145.
(69) Li, Y.; Lin, M.; Davenport, J. W. *J. Phys. Chem. C* **2011**, *115*, 11533–11539.
(70) Hartigan, J. A. *Clustering Algorithms*; John Wiley & Sons, Inc.: New York, 1975. Hess, B.; Kutzner, C.; van der Spoel, D.; Lindahl, E. *J. Chem. Theory Comput.* **2008**, *4*, 435.
(71) Bučko, T. s.; Hafner, J. r.; Lebègue, S. b.; Ángyán, J. n. G. *J. Phys. Chem. A* **2010**, *114*, 11814.
(72) Frisch, M. J., et al. *Gaussian09, revision A.1*; Gaussian, Inc.: Wallingford, CT, 2009.
(73) Zhao, Y.; Truhlar, D. G. *Theor. Chem. Acc.* **2008**, *120*, 215–241. Zhao, Y.; Schultz, N. E.; Truhlar, D. G. *J. Chem. Theory Comput.* **2006**, *2*, 364–382. Zhao, Y.; Truhlar, D. G. *J. Chem. Theory Comput.* **2006**, *2*, 1009–1018.
(74) Zhao, Y.; Truhlar, D. G. *J. Am. Chem. Soc.* **2007**, *129*, 8440–8442.
(75) Zhao, Y.; Truhlar, D. G. *J. Chem. Theory Comput.* **2007**, *3*, 289–300.
(76) Tishchenko, O.; Zheng, J. J.; Truhlar, D. G. *J. Chem. Theory Comput.* **2008**, *4*, 1208–1219.
(77) Truhlar, D. G. *J. Am. Chem. Soc.* **2008**, *130*, 16824–16827.
(78) Valero, R.; Costa, R.; Moreira, I.; Truhlar, D. G.; Illas, F. *J. Chem. Phys.* **2008**, 128.
(79) Jacquemin, D.; Perpete, E. A.; Ciofini, I.; Adamo, C.; Valero, R.; Zhao, Y.; Truhlar, D. G. *J. Chem. Theory Comput.* **2010**, *6*, 2071–2085.
(80) Hohenstein, E. G.; Chill, S. T.; Sherrill, C. D. *J. Chem. Theory Comput.* **2008**, *4*, 1996–2000.
(81) Bader, R. F. W. *Atoms in Molecules: A Quantum Theory*; Clarendon Press: Oxford, UK, 1990.
(82) Biegler-Konig, F.; Schonbohm, J.; Derdau, R.; Bayles, D.; Bader, R. F. W. *AIM2000, version 1*; Bielefeld: Germany, 2000.
(83) Boys, S. F.; Bernardi, F. *Mol. Phys.* **1970**, *19*, 553–566.
(84) Bryantsev, V. S.; Diallo, M. S.; van Duin, A. C. T.; Goddard, W. A. *J. Chem. Theory Comput.* **2009**, *5*, 1016–1026.
(85) Grabowski, S. J. *J. Mol. Struct.* **2001**, *562*, 137–143. Grabowski, S. J. *J. Phys. Org. Chem.* **2004**, *17*, 18–31.
(86) Grabowski, S. J.; Malecka, M. *J. Phys. Chem. A* **2006**, *110*, 11847–11854.
(87) Grabowski, S. J.; Sokalski, W. A.; Dyguda, E.; Leszczynski, J. *J. Phys. Chem. B* **2006**, *110*, 6444–6446.
(88) Grabowski, S. J.; Sokalski, W. A.; Leszczynski, J. *J. Phys. Chem. A* **2005**, *109*, 4331–4341.
(89) Parthasarathi, R.; Tian, J.; Redondo, A.; Gnanakaran, S. *J. Phys. Chem. A* **2011**, *115*, 12826–12840.
(90) Matta, C. F.; Hernandez-Trujillo, J.; Tang, T. H.; Bader, R. F. W. *Chem.—Eur. J.* **2003**, *9*, 1940–1951.
(91) Parthasarathi, R.; Amutha, R.; Subramanian, V.; Nair, B. U.; Ramasami, T. *J. Phys. Chem. A* **2004**, *108*, 3817–3828.
(92) Parthasarathi, R.; Raman, S. S.; Subramanian, V.; Ramasami, T. *J. Phys. Chem. A* **2007**, *111*, 7141–7148.
(93) Parthasarathi, R.; Subramanian, V. *Chem. Phys. Lett.* **2006**, *418*, 530–534.
(94) Ziolkowski, M.; Grabowski, S. J.; Leszczynski, J. *J. Phys. Chem. A* **2006**, *110*, 6514–6521.
(95) Koch, U.; Popelier, P. L. A. *J. Phys. Chem.* **1995**, *99*, 9747–9754.

(96) Parthasarathi, R.; Elango, M.; Subramanian, V.; Sathyamurthy, N. *J. Phys. Chem. A* **2009**, *113*, 3744–3749.
(97) Mandal, A.; Prakash, M.; Kumar, R. M.; Parthasarathi, R.; Subramanian, V. *J. Phys. Chem. A* **2010**, *114*, 2250.
(98) Parthasarathi, R.; Subramanian, V.; Sathyamurthy, N. *J. Phys. Chem. A* **2006**, *110*, 3349–3351.
(99) Parthasarathi, R.; Subramanian, V.; Sathyamurthy, N. *J. Phys. Chem. A* **2007**, *111*, 13287–13290.
(100) Parthasarathi, R.; Subramanian, V.; Sathyamurthy, N. *Synth. React. Inorg. Met.-Org. Nano-Met. Chem.* **2008**, *38*, 18–26.
(101) Matta, C. F., Boyd, R. J., Eds.; *The Quantum Theory of Atoms in Molecules: Fom Solid State to DNA and Drug Design*; Wiley-VCH: Weinheim, Germany, 2007.
(102) Gadre, S. R.; Shirsat, R. N. *Electrostatics of Atoms and Molecules*; Universities Press: Hyderabad, India, 2000.
(103) Muhletha., K *Ann. Rev. Plant Physiol.* **1967**, *18*, 1.
(104) Lehtiö, J.; Sugiyama, J.; Gustavsson, M.; Fransson, L.; Linder, M.; Teeri, T. T. *Proc. Natl. Acad. Sci. U.S.A.* **2003**, *100*, 484–489.
(105) Beckham, G. T.; Matthews, J. F.; Bomble, Y. J.; Bu, L.; Adney, W. S.; Himmel, M. E.; Nimlos, M. R.; Crowley, M. F. *J. Phys. Chem. B* **2010**, *114*, 1447–1453.
(106) Mormann, W.; Wagner, T. *Carbohydr. Polym.* **2000**, *43*, 257–262.
(107) Schleicher, H.; Daniels, C.; Philipp, B. *J. Polym. Sci.: Polym. Symp.* **1974**, *47*, 251–260.